axioms

MDPI

Article

Chaotic Dynamics by Some Quadratic Jerk Systems

Mei Liu [1], Bo Sang [1,*], Ning Wang [2] and Irfan Ahmad [3]

[1] School of Mathematical Sciences, Liaocheng University, Liaocheng 252059, China; liumei_a@163.com
[2] School of Electrical and Information Engineering, Tianjin University, Tianjin 300072, China; cczuwangning@163.com
[3] Sirindhorn International Institute of Technology, Thammasat University, Pathum Thani 12000, Thailand; irfan.ahmad2691@gmail.com
* Correspondence: sangbo_76@163.com

Abstract: This paper is about the dynamical evolution of a family of chaotic jerk systems, which have different attractors for varying values of parameter a. By using Hopf bifurcation analysis, bifurcation diagrams, Lyapunov exponents, and cross sections, both self-excited and hidden attractors are explored. The self-exited chaotic attractors are found via a supercritical Hopf bifurcation and period-doubling cascades to chaos. The hidden chaotic attractors (related to a subcritical Hopf bifurcation, and with a unique stable equilibrium) are also found via period-doubling cascades to chaos. A circuit implementation is presented for the hidden chaotic attractor. The methods used in this paper will help understand and predict the chaotic dynamics of quadratic jerk systems.

Keywords: Hopf bifurcation; limit cycle; period-doubling cascade; self-excited attractor; hidden attractor

check for updates

Citation: Liu, M.; Sang, B.; Wang, N.; Ahmad, I. Chaotic Dynamics by Some Quadratic Jerk Systems. *Axioms* **2021**, *10*, 227. https://doi.org/10.3390/axioms10030227

Academic Editors: Omar Bazighifan, Maria Alessandra Ragusa and Fahd Jarad

Received: 1 August 2021
Accepted: 6 September 2021
Published: 14 September 2021

Publisher's Note: MDPI stays neutral with regard to jurisdictional claims in published maps and institutional affiliations.

Copyright: © 2021 by the authors. Licensee MDPI, Basel, Switzerland. This article is an open access article distributed under the terms and conditions of the Creative Commons Attribution (CC BY) license (https://creativecommons.org/licenses/by/4.0/).

1. Introduction

It is believed that a wide variety of natural phenomena are chaotic, including fluid flow, heartbeat irregularities, weather, and climate [1]. A dynamical system displaying sensitive dependence on initial conditions on a closed invariant set (which consists of more than one orbit) is called chaotic [2]. Chaos theory has applications in a variety of fields, including disease control and prevention [3], mechanics [1,4], biology [5], cryptography [6], secure communications [7], etc. In the study of chaos theory and its applications, it is very important to identify new chaotic systems or enhance the complexity of dynamics and shapes of chaotic attractors based on existing ones [8].

According to Leonov et al. [9], the attractors in dynamical systems are categorized as self-excited attractors and hidden attractors. A self-excited attractor has a basin of attraction that is associated with an unstable equilibrium. Conversely, an attractor is called hidden if its basin of attraction does not intersect with a small neighborhood of any equilibrium point.

Since the discovery of a chaotic system by Lorenz in 1963 [10], many other chaotic systems have been found and studied, such as the Rössler system [11], the Chua circuit [12,13], chaotic jerk circuit [14], the Chen system [15], the Lü system [16], and the Sprott systems [17]. These examples have one or more saddle-points and the associated attractors in these papers are all self-excited. Since the basin of attraction of a self-excited attractor is associated with an unstable equilibrium, self-excited attractors can be localized numerically by the standard computational procedure: after a transient process, a trajectory that starts in the neighborhood of an unstable equilibrium (from a point on its unstable manifold) is attracted to the attractor and traces it [9].

For numerical localization of hidden attractors, it needs to develop special analytical-numerical procedures, since there are no transient processes leading to such attractors from the neighborhoods of the unstable equilibria. An analytical-numerical algorithm has been proposed by Leonov et al. [18,19]. Examples of hidden attractors based on this algorithm can be found in [9,19–22]. Sprott et al. found some hidden chaotic attractors

with an exhaustive computer search [23–28]. Recently, researchers have proposed many dynamical systems with hidden attractors, see [20,25,28–33]. Hidden attractors may be found in the following three families: (1) systems without equilibrium, see [23,34–39]; (2) systems with stable equilibrium, see [21,40–46]; (3) systems with an infinite number of equilibria, see [24,26,27,47–49]. Pham et al. [50–52] explored the relationships among these three families with hidden attractors. Many hidden attractors have been found in some jerk systems [23,42,53–56]. Hidden attractors in fractional order systems were also studied in [57,58].

In nonlinear dynamical systems, multistability refers to the coexistence of different stable states [25,29,35,43,59]. Multistable dynamical systems are very sensitive to noise, initial conditions, and system parameters [60–64]. Although multistability increases the difficulty of some engineering constructions, such as bridge vibration and wing design, chaotic systems with multistability are very useful in the field of secure communication [65,66]. It has been shown that multistability is connected with the occurrence of hidden attractors [67–69]. In particular, systems with stable equilibrium and hidden attractors are examples of multistable systems [21,40–46]. The coexisting self-excited attractors in multistable systems can be found using the standard computational procedure, whereas there is no standard method for predicting the existence or coexistence of hidden attractors in a system [20]. Some jerk systems and hyperjerk systems with multistability and chaotic dynamics have been found: self-excited chaos [63,70,71], hidden chaos [56,72].

The paper is organized as follows. In Section 2, for a five-parameter family of quadratic jerk systems, the Hopf bifurcation is analyzed via the first order focus quantity. In Section 3, a two-parameter family is presented, which can be embedded in the previous five-parameter family. The remaining sections are devoted to the two-parameter family. In Section 4, the nonchaotic parameter region is discussed. In Section 5, the Hopf bifurcation is analyzed for the family with two parameters. In Sections 6 and 7, the routes to chaos are numerically studied for self-excited and hidden attractors, respectively. In Section 8, an elegant hidden chaotic flow is introduced and analyzed. In Section 9, a circuit implementation is presented to model the hidden chaotic system. Finally, in Section 10, the conclusions are presented.

2. Hopf Bifurcation of a Five-Parameter Family of Quadratic Jerk Systems

In physics, jerk is the third derivative of position with respect to time. Therefore, differential equations of the form

$$\dddot{x} = J(x, \dot{x}, \ddot{x}) \tag{1}$$

are called jerk equations. As usual, the over-dot represents the derivative of the variable with respect to t.

Letting $y = \dot{x}, z = \ddot{x}$, Equation (1) can be transformed into the following jerk system

$$\begin{cases} \dfrac{dx}{dt} = y, \\ \dfrac{dy}{dt} = z, \\ \dfrac{dz}{dt} = J(x, y, z), \end{cases} \tag{2}$$

which can exhibit many features of regular and chaotic motions. The study of chaos (either self-excited or hidden) in jerk systems has attracted significant attention in [8,17,23,42,70,73,74].

By considering many thousands of combinations of the coefficients, Molaie, Jafari and Sprott [42] identified 23 chaotic flows with a stable equilibrium, in which the cases SE_1–SE_6 are some elegant quadratic jerk systems. Let us recall the first case SE_1:

$$\begin{cases} \dfrac{dx}{dt} = y, \\ \dfrac{dy}{dt} = z, \\ \dfrac{dz}{dt} = -x - 0.6\,y - 2\,z + z^2 - 0.4\,xy, \end{cases} \tag{3}$$

which is an elegant system within the five-parameter family of jerk systems:

$$\begin{cases} \dfrac{dx}{dt} = y, \\ \dfrac{dy}{dt} = z, \\ \dfrac{dz}{dt} = -a_1\,x - a_2\,y - a_3\,z + a_4\,z^2 + a_5\,xy, \end{cases} \tag{4}$$

where $a_1, a_2, \cdots, a_5$ are real parameters. For system (3), the initial conditions used in [42] are $x(0) = 4$, $y(0) = -2$ and $z(0) = 0$.

By "elegant", it means that as many coefficients as possible are set to zero with the others to ± 1, if possible, or to a small integer or decimal fraction with the fewest possible digits [42,75]. The other cases SE_2–SE_6 are not in this family. Although so many combinations of the coefficients have been used, there are still some more elegant chaotic flows (with a stable equilibrium) that need to be found for the family. For the flow, the transition to chaos should be understood via bifurcation theory.

For $a_1 \neq 0$, system (4) has a unique equilibrium at the origin. The type of this equilibrium depends on the parameters a_1, a_2 and a_3 of the third equation. The characteristic polynomial of the jacobian matrix at the origin is

$$g(\lambda) = \lambda^3 + a_3\,\lambda^2 + a_2\,\lambda + a_1. \tag{5}$$

whose discriminant with respect to λ is

$$\Delta = -4a_1a_3^3 + a_2^2a_3^2 + 18a_1a_2a_3 - 4a_2^3 - 27a_1^2.$$

It is well known that the occurrence of Hopf bifurcation may be associated with the birth of a strange attractor: self-excited or hidden, for more information see [21,76]. The following situation is of interest for us:

$$a_1 > 0, a_2 > 0, a_3 > 0, \Delta < 0. \tag{6}$$

By setting (5) to zero, an application of the implicit function theorem yields the transversality condition:

$$\begin{aligned} \left.\frac{d\,\mathrm{Re}\,\lambda_{1,2}}{da}\right|_{a_1=a_2a_3} &= \left.\frac{-1}{3\lambda^2 + 2\,a_3\lambda + a_2}\right|_{\lambda=\pm\sqrt{a_2}\mathrm{i}} \\ &= \frac{1}{2\left(a_2 + a_3^2\right)} > 0. \end{aligned} \tag{7}$$

In view of (6) and (7), according to [77], a Hopf bifurcation occurs at $a_1 = a_2a_3$.

Setting $a_1 = a_2 a_3$ and

$$\begin{cases} x = -\dfrac{u}{a_2} - \dfrac{v}{a_2} + \dfrac{w}{a_3^2}, \\ y = -\dfrac{\mathrm{i}u}{\sqrt{a_2}} + \dfrac{\mathrm{i}v}{\sqrt{a_2}} - \dfrac{w}{a_3}, \\ z = u + v + w, \end{cases} \tag{8}$$

system (4) becomes

$$\begin{cases} \dfrac{du}{dt} = \mathrm{i}\sqrt{a_2}\, u + c^{(1)}_{2,0,0} u^2 + c^{(1)}_{1,1,0} uv + c^{(1)}_{0,2,0} v^2 + c^{(1)}_{1,0,1} uw + c^{(1)}_{0,1,1} vw + c^{(1)}_{0,0,2} w^2, \\ \dfrac{dv}{dt} = -\mathrm{i}\sqrt{a_2}\, v + c^{(2)}_{2,0,0} u^2 + c^{(2)}_{1,1,0} uv + c^{(2)}_{0,2,0} v^2 + c^{(2)}_{1,0,1} uw + c^{(2)}_{0,1,1} vw + c^{(2)}_{0,0,2} w^2, \\ \dfrac{dw}{dt} = -a_3 w + d_{2,0,0} u^2 + d_{1,1,0} uv + d_{0,2,0} v^2 + d_{1,0,1} uw + d_{0,1,1} vw + d_{0,0,2} w^2, \end{cases} \tag{9}$$

where

$$\overline{c^{(1)}_{p_1,p_2,q}} = c^{(2)}_{p_2,p_1,q}, \quad \overline{d_{p_1,p_2,q}} = d_{p_2,p_1,q},$$

and

$$\begin{aligned}
c^{(1)}_{2,0,0} &= \frac{a_2^2 a_4 - a_3 a_5}{2a_2\left(a_3^2 + a_2\right)} + \frac{a_2 a_3 a_4 + a_5}{2\sqrt{a_2}\left(a_3^2 + a_2\right)}\,\mathrm{i}, \\
c^{(1)}_{1,1,0} &= \frac{a_2 a_4}{a_3^2 + a_2} + \frac{a_3\sqrt{a_2}\, a_4}{a_3^2 + a_2}\,\mathrm{i}, \\
c^{(1)}_{0,2,0} &= \frac{a_2^2 a_4 + a_3 a_5}{2a_2\left(a_3^2 + a_2\right)} + \frac{a_2 a_3 a_4 - a_5}{2\sqrt{a_2}\left(a_3^2 + a_2\right)}\,\mathrm{i}, \\
c^{(1)}_{1,0,1} &= \frac{a_2 a_3 a_4 + a_5}{a_3\left(a_3^2 + a_2\right)} + \frac{2a_2 a_3^3 a_4 + a_3^2 a_5 - a_2 a_5}{2\sqrt{a_2}\, a_3^2\left(a_3^2 + a_2\right)}\,\mathrm{i}, \\
c^{(1)}_{0,1,1} &= \frac{a_2 a_4}{a_3^2 + a_2} + \frac{2a_2 a_3^3 a_4 + a_3^2 a_5 + a_2 a_5}{2\sqrt{a_2}\, a_3^2\left(a_3^2 + a_2\right)}\,\mathrm{i}, \\
c^{(1)}_{0,0,2} &= \frac{a_2\left(a_3^3 a_4 - a_5\right)}{2\left(a_3^2 + a_2\right)a_3^3} + \frac{\sqrt{a_2}\left(a_3^3 a_4 - a_5\right)}{2a_3^2\left(a_3^2 + a_2\right)}\,\mathrm{i}, \\
d_{2,0,0} &= \frac{a_3^2 a_4}{a_3^2 + a_2} + \frac{a_3^2 a_5}{\left(a_3^2 + a_2\right)a_2^{\frac{3}{2}}}\,\mathrm{i}, \\
d_{1,1,0} &= \frac{2a_3^2 a_4}{a_3^2 + a_2}, \\
d_{1,0,1} &= \frac{a_3\left(2a_2 a_3 a_4 + a_5\right)}{a_2\left(a_3^2 + a_2\right)} - \frac{a_5}{\sqrt{a_2}\left(a_3^2 + a_2\right)}\,\mathrm{i}, \\
d_{0,0,2} &= \frac{a_3^3 a_4 - a_5}{a_3\left(a_3^2 + a_2\right)}.
\end{aligned}$$

Let us consider the general system

$$\begin{cases} \dfrac{du}{dt} = \mathrm{i}\omega u + \displaystyle\sum_{p_1+p_2+q=2}^{\infty} a^{(1)}_{p_1,p_2,q} u^{p_1} v^{p_2} w^q = U(u,v,w), \\ \dfrac{dv}{dt} = -\mathrm{i}\omega v + \displaystyle\sum_{p_1+p_2+q=2}^{\infty} a^{(2)}_{p_1,p_2,q} u^{p_1} v^{p_2} w^q = V(u,v,w), \\ \dfrac{dw}{dt} = -\delta w + \displaystyle\sum_{p_1+p_2+q=2}^{\infty} b_{p_1,p_2,q} u^{p_1} v^{p_2} w^q = W(u,v,w), \end{cases} \tag{10}$$

where

$$\overline{a^{(1)}_{p_1,p_2,q}} = a^{(2)}_{p_2,p_1,q}, \quad \overline{b_{p_1,p_2,q}} = b_{p_2,p_1,q}, \quad \omega > 0, \quad \delta > 0.$$

According to [78], for system (10), one can derive successively the terms of the following formal series:

$$F(u,v,w) = uv + \sum_{s=3}^{\infty}\sum_{k=0}^{s}\sum_{j=0}^{s-k} M_{s,k,j} u^{s-k-j} v^k w^j,$$

such that

$$\frac{dF}{dt}\Big|_{(10)} = \frac{\partial F}{\partial u}U + \frac{\partial F}{\partial v}V + \frac{\partial F}{\partial w}W = \sum_{n=1}^{\infty} W_n (uv)^{n+1}, \tag{11}$$

where $M_{s,k,j}$ can be uniquely determined by setting $M_{2m,m,0} = 0$ for $m \geq 2$.

Definition 1 ([79])**.** *The coefficients W_n of the formal series (11) are called the n-th order focus quantities of system (10).*

Consider a family of quadratic systems in the form of (10), i.e.,

$$\begin{cases} \dfrac{du}{dt} = \alpha_1 u + \alpha_2 u^2 + \alpha_3 uv + \alpha_4 v^2 + \alpha_5 uw + \alpha_6 vw + \alpha_7 w^2, \\ \dfrac{dv}{dt} = -\alpha_1 v + \beta_2 u^2 + \beta_3 uv + \beta_4 v^2 + \beta_5 uw + \beta_6 vw + \beta_7 w^2, \\ \dfrac{dw}{dt} = \delta_1 w + \delta_2 u^2 + \delta_3 uv + \delta_4 v^2 + \delta_5 uw + \delta_6 vw + \delta_7 w^2, \end{cases} \tag{12}$$

where $\alpha_1 = \omega \mathtt{i}$ with $\omega > 0$, $\delta_1 < 0$.

Lemma 1 ([79])**.** *For system (12), the first order focus quantity of the origin is*

$$W_1 = \frac{W_{1,1}}{-4\,{\alpha_1}^3\delta_1 + \alpha_1{\delta_1}^3}, \tag{13}$$

where

$$\begin{aligned} W_{1,1} \;=\; & -4\,\delta_3(\alpha_5+\beta_6){\alpha_1}^3 - 2\,\delta_1(2\,\alpha_2\alpha_3 - \delta_2\alpha_6 - 2\,\beta_3\beta_4 + \delta_4\beta_5){\alpha_1}^2 \\ & + {\delta_1}^2(\alpha_5\delta_3 + \delta_2\alpha_6 + \delta_4\beta_5 + \beta_6\delta_3)\alpha_1 + {\delta_1}^3(\alpha_2\alpha_3 - \beta_3\beta_4). \end{aligned}$$

Theorem 1. *For system (4) with $a_1 = a_2a_3$, the first order focus quantity of the origin is*

$$W_1 = \frac{8a_2^3a_3a_4^2 - a_2a_3^2a_4a_5 + 14a_2^2a_4a_5 - a_3a_5^2}{\left(a_3^2+4a_2\right)\left(a_3^2+a_2\right)a_2^2}. \tag{14}$$

Letting

$$I = 8a_2^3a_3a_4^2 - a_2a_3^2a_4a_5 + 14a_2^2a_4a_5 - a_3a_5^2 \tag{15}$$

be the numerator of W_1 and $a_2 > 0, a_3 > 0$, the Hopf bifurcation occurs at $a_1 = a_2a_3$ is supercritcal if $I < 0$, and subcritical if $I > 0$.

Proof. Recall that for system (4), $a_1 = a_2a_3$ is the bifurcation value of the Hopf bifurcation. Note that system (9) is obtained from system (4) (with $a_1 = a_2a_3$) via the non-degenerate change of coordinates (8).

An application of the formula (13) to the transformed system (9) yields the first order focus quantity W_1 shown in (14), whose sign determines the criticality of Hopf bifurcation. In view of $a_2 > 0, a_3 > 0$ and the transversality condition (7), the bifurcation is supercritical if $I < 0$, and subcritical if $I > 0$. In the supercritical case, the bifurcation generates a family

of stable limit cycles for $a_1 > a_2a_3$, while in the subcritical case, it generates a family of unstable limit cycles for $a_1 < a_2a_3$. □

Before discussing the transition to chaos, the local stability of the origin under the conditions (6) needs to be discussed. Applying the Routh–Hurwitz criterion to (5) yields:

- For $a_1 > a_2a_3$, the origin is unstable. Moreover, it is a saddle-focus of the type (1,2) with 1D stable and 2D unstable manifolds [21].
- For $a_1 < a_2a_3$, the origin is asymptotically stable. Moreover, it is a node-focus.

Now let us vary the parameter a_1 and discuss the transition to chaos. For the case $W_1 < 0$, if there exists a period doubling route to chaos with the increase in a_1 in some subset of $(a_2a_3, +\infty)$, self-excited chaotic attractors can be found for certain values of a_1. For the case $W_1 > 0$, if there exists a reverse period doubling route to chaos with the decrease in a_1 in some subset of $(0, a_2a_3)$, hidden chaotic attractors can be found for certain values of a_1. This idea is straightforward, from which some elegant chaotic flows can be constructed.

3. The Proposed Systems

In order to find algebraically simple chaotic systems, a family of quadratic jerk systems

$$\begin{cases} \dfrac{dx}{dt} = y, \\ \dfrac{dy}{dt} = z, \\ \dfrac{dz}{dt} = -a\,x - y - 1.1\,z - \alpha\,z^2 + xy, \end{cases} \tag{16}$$

is considered, where $a, \alpha \in \mathbb{R}$. It is a special case of system (4) with $a_2 = a_5 = 1$, $a_3 = 1.1$, $a_1 = a$ and $a_4 = -\alpha$.

The system does not admit the common symmetries: symmetric with respect to the origin, symmetric with respect to the coordinate planes, and many other symmetries. In fact, the system is slightly modified from the following system

$$\begin{cases} \dfrac{dx}{dt} = y, \\ \dfrac{dy}{dt} = z, \\ \dfrac{dz}{dt} = -a\,x - y - 1.1\,z - \alpha\,z^2, \end{cases} \tag{17}$$

which is invariant under the transformation $(x, y, z, \alpha) \to (-x, -y, -z, -\alpha)$. However, for system (16), the presence of the cross term xy in the third equation breaks the symmetry.

The divergence of flow of the system (16) is calculated as

$$\nabla V = -1.1 - 2\alpha z,$$

If $\nabla V < 0$, i.e., $1.1 + 2\alpha z > 0$ (on average) in some region, the phase space volume contracts and the system is dissipative. In particular, if $\nabla V \equiv -1.1$, i.e., $\alpha = 0$, system (16) is dissipative; moreover, the exponential contraction rate is calculated as follows

$$\frac{dV}{dt} = -1.1\,V \Rightarrow V = V(0)e^{-1.1t}, \tag{18}$$

thus each volume containing the system trajectory shrinks to zero as $t \to \infty$ at an exponential rate of $-1.1t$.

In this paper, for fixed α, the parameter a is selected as the bifurcation parameter. By performing bifurcation analysis, the dynamical evolution of system (16) from simple to complex structures will be investigated.

4. Nonchaotic Parameter Region

In some cases, system (16) can not have chaotic solutions.

Theorem 2. *For $\alpha = 0, a \leq 0$, system (16) does not have bounded chaotic solutions.*

Proof. In this case, system (16) is equivalent to the following third order equation

$$\dddot{x} = -a\,x - \dot{x} - 1.1\,\ddot{x} + x\dot{x}, \tag{19}$$

where $a \leq 0$ and $\dot{x} = y, \ddot{x} = z$.

Multiplying both sides of Equation (19) by x yields

$$x\dddot{x} = -a\,x^2 - x\dot{x} - 1.1\,x\ddot{x} + x^2\dot{x}.$$

Integrating the equation with respect to t gives

$$x\ddot{x} - \frac{1}{2}\dot{x}^2 + \frac{1}{2}x^2 + 1.1\,x\dot{x} - \frac{1}{3}x^3 = C + \int_0^t (-a\,x^2 + 1.1\,\dot{x}^2)dt. \tag{20}$$

Substituting $\dot{x} = y, \ddot{x} = z$ into (20) produces

$$xz - \frac{1}{2}y^2 + \frac{1}{2}x^2 + 1.1\,xy - \frac{1}{3}x^3 = C + \int_0^t (-a\,x^2 + 1.1\,y^2)dt. \tag{21}$$

Since $a \leq 0$, Equation (21) has a monotone left-hand side. Let $P(x, y, z)$ be the left-hand side of Equation (21). The polynomial $P(x, y, z)$, as a function of time, has a limit $L \in \mathbb{R}$ as t tends to infinity. If L is finite, then any attractor of system (16) lies on the two-dimensional surface $P(x, y, z) = K$, where K is a constant, and thus is not chaotic due to the Poincaré–Bendixson theorem. If $L = \pm\infty$, then at least one of the variables is not bounded and cannot be chaotic. This completes the proof. □

Remark 1. *For $\alpha = a = 0$, system (16) admits a polynomial first integral*

$$F(x, y, z) = -\frac{1}{2}x^2 + x + 1.1\,y + z.$$

Thus, the phase space is foliated by a family of invariant algebraic surfaces $F(x, y, z) = C$. Hence, the system is not chaotic.

5. Hopf Bifurcation Analysis

The characteristic polynomial of the jacobian matrix of system (16) at the origin is

$$g(\lambda) = \lambda^3 + 1.1\lambda^2 + \lambda + a, \tag{22}$$

whose discriminant with respect to λ is

$$\Delta = -27a^2 + \frac{3619}{250}a - \frac{279}{100}.$$

It should be noted that Δ is negative for all $a \in \mathbb{R}$.

For now, the parameter a is assumed to be positive. Thus, the polynomial (22) has a pair of complex conjugate roots $\lambda_{1,2} = \lambda_{1,2}(a)$ and one negative root $\lambda_3 = \lambda_3(a)$. Let $k = \operatorname{Re}\lambda_{1,2}$. The variation of k with respect to a is presented in Figure 1. In the range $0 < a < 1.1$, it follows that $k < 0$; and in the range $a > 1.1$, it follows that $k > 0$. Indeed, there is a simple root at $a = 1.1$. There are three possibilities for the origin: for $a > 1.1$, the origin is a saddle-focus of the type (1,2) with 1D stable and 2D unstable manifolds; when $a = 1.1$, the origin is a non-hyperbolic equilibrium; for $0 < a < 1.1$, the origin is a stable node-focus.

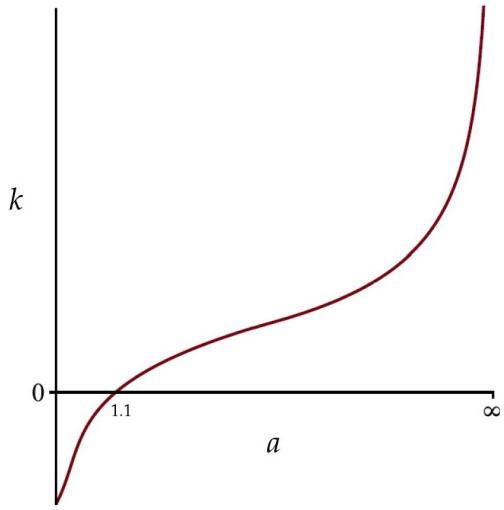

Figure 1. The curve $k = k(a)$ with $a \in (0, \infty)$.

Theorem 3. *For system* (16)*, a Hopf bifurcation occurs at the critical value* $a = 1.1$ *for the origin. For* $\alpha \in (-0.0814411693, 1.534850260)$*, the bifurcation is supercritical; for* $\alpha \in (-\infty, -0.0814411693) \cup (1.534850260, +\infty)$*, the bifurcation is subcritical.*

Proof. The first assertion follows directly from the existence of a Hopf bifurcation in the general system (4), because system (16) is a special system of (4). For more information, see Section 2.

By setting $a_1 = a = 1.1$ and $a_2 = a_5 = 1$, $a_3 = 1.1$, $a_4 = -\alpha$ in (14), the first order focus quantity of system (16) is obtained as

$$W_1 = \frac{88000}{115141}\alpha^2 - \frac{127900}{115141}\alpha - \frac{11000}{115141}.$$

For $\alpha \in (-0.0814411693, 1.534850260)$, i.e., $W_1 < 0$, the Hopf bifurcation is supercritical, giving rise to a family of stable limit cycles for $a > 1.1$.

For $\alpha \in (-\infty, -0.0814411693) \cup (1.534850260, +\infty)$, i.e., $W_1 > 0$, the Hopf bifurcation is subcritical, giving rise to a family of unstable limit cycles for $a < 1.1$. □

Remark 2. *The limit cycles arising from the supercritical Hopf bifurcation can help to find a self-excited chaotic attractor; for more details, see Section* 6*.*

Remark 3. *According to the conjecture in [21], subcritical Hopf bifurcations may lead to the birth of hidden attractors. In the current paper, see Section* 7*.*

Remark 4. *Assume that* $a < 0$*. Then the polynomial* (22) *has two complex conjugate roots* $\lambda_{1,2} = \lambda_{1,2}(a)$ *and one positive root* $\lambda_3 = \lambda_3(a)$*.*

Since

$$\begin{aligned} \lambda_1 + \lambda_2 &= 2\,\mathrm{Re}\,\lambda_{1,2}, \\ \lambda_1 + \lambda_2 + \lambda_3 &= -1.1, \qquad \lambda_3 > 0, \end{aligned}$$

it follows that $\mathrm{Re}\,\lambda_{1,2} < 0$*. Thus, the origin is a hyperbolic saddle-focus of the type (2,1) with 2D stable and 1D unstable manifolds [21].*

6. Route to a Self-Excited Chaotic Attractor

For system (16) with $\alpha = 0.3$ and $a = 1.1$, the first order focus quantity W_1 is negative. Thus a supercritical Hopf bifurcation occurs at $a = 1.1$, giving rise to a family of stable limit cycles for $a > 1.1$.

With $\alpha = 0.3$ and initial condition $(0.1, 0.1, 0.1)$, the parameter a is varied in the region of [0.9,2.3]. The bifurcation diagram of system (16) depicting the local maxima of $x(t)$ is presented in Figure 2a. When the parameter a varies from 0.9 to 2.3, the system displays no oscillation up to $a = 1.1$ where the Hopf bifurcation triggers a period-1 limit cycle. With further increase in parameter a, the component $x(t)$ shows a period-doubling route to chaotic oscillations interspersed with periodic windows. The corresponding Lyapunov exponents versus a are shown in Figure 2b.

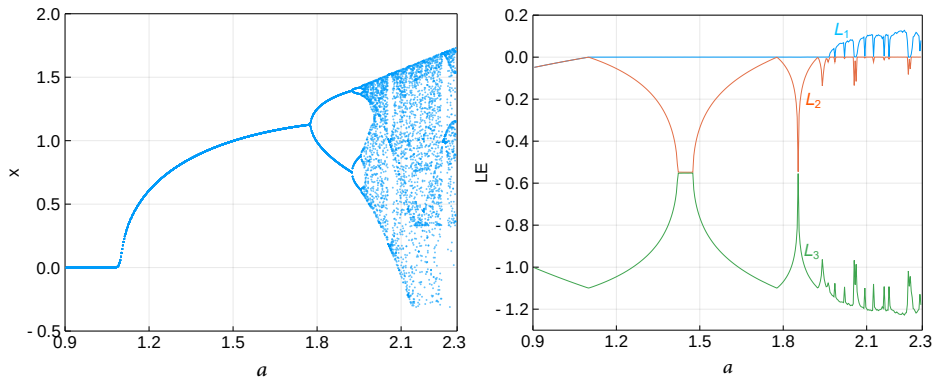

(**a**) (**b**)

Figure 2. (**a**) Bifurcation diagram, and (**b**) Lyapunov exponents spectrum versus a of system (16).

For $a = 2, \alpha = 0.3$, system (16) becomes

$$\begin{cases} \dfrac{dx}{dt} = y, \\ \dfrac{dy}{dt} = z, \\ \dfrac{dz}{dt} = -2x - y - 1.1z - 0.3z^2 + xy. \end{cases} \tag{23}$$

A chaotic attractor of system (23) is shown in Figure 3.

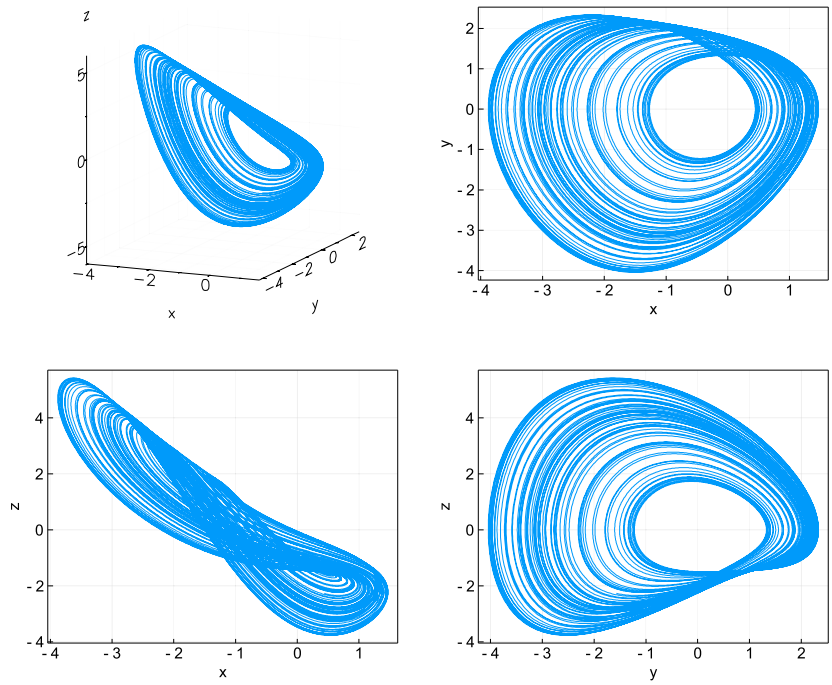

Figure 3. Self-excited chaotic attractor (in blue) of system (16) with $a = 2$, $\alpha = 0.3$ for the initial condition $(0.1, 0.1, 0.1)$.

By Section 5, the unique equilibrium located at the origin is unstable, so that the attractor is self-excited. The Lyapunov exponents of the attractor are $(L_1, L_2, L_3) = (0.06427, 0.0002449, -1.1645)$, thus the Kaplan–Yorke dimension is $D_{KY} = 2.0554$. This confirms that system (23) is dissipative with a self-excited chaotic attractor. Figure 4 shows the cross sections of the basin of attraction of the attractor in the three coordinate planes.

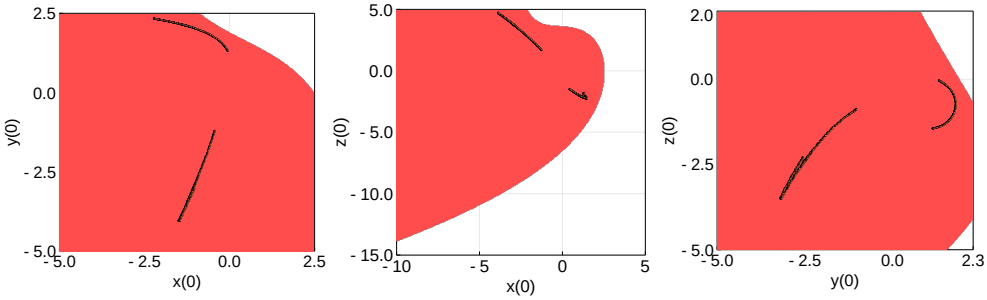

Figure 4. Cross sections of the basin of attraction of the chaotic attractor in the planes: $z(0) = 0$ (**left**); $y(0) = 0$ (**center**); $x(0) = 0$ (**right**). Initial conditions in the white regions lead to unbounded orbits, and those in the red regions lead to the chaotic attractor.

7. Route to a Hidden Chaotic Attractor

Consider the general system

$$\begin{cases} \dfrac{dx}{dt} = y, \\ \dfrac{dy}{dt} = z, \\ \dfrac{dz}{dt} = -a\,x - y - 1.1\,z - \alpha\,z^2 + x(y + \beta\,z), \end{cases} \tag{24}$$

where $a > 0, \alpha, \beta \in \mathbb{R}$. It has a unique equilibrium at the origin. Note that if $\beta = 0$, system (24) is reduced to system (16).

Since the characteristic polynomial of system (24) is also (22), there are three possibilities for the origin: for $a > 1.1$, the origin is a saddle-focus of the type (1,2) with 1D stable and 2D unstable manifolds; for $a = 1.1$, the origin is a non-hyperbolic equilibrium; for $0 < a < 1.1$, the origin is a stable node-focus. Furthermore, a Hopf bifurcation occurs at the critical value $a = 1.1$ for the origin. Letting $a = 1.1$, it is routine [79] to compute the first order focus quantity W_1 of system (24) at the origin. The result is

$$W_1 = \frac{88000\alpha^2}{115141} + \frac{(531000\beta - 1406900)\alpha}{1266551} - \frac{437000\beta^2}{1266551} - \frac{120000\beta}{115141} - \frac{11000}{115141}.$$

For $\alpha = 2.9, \beta = 1$; $\alpha = 2.7, \beta = 0.25$; $\alpha = 2.59, \beta = 0$, system (24) becomes

$$\begin{cases} \dfrac{dx}{dt} = y, \\ \dfrac{dy}{dt} = z, \\ \dfrac{dz}{dt} = -a\,x - y - 1.1\,z - 2.9\,z^2 + x(y + z), \end{cases} \tag{25}$$

$$\begin{cases} \dfrac{dx}{dt} = y, \\ \dfrac{dy}{dt} = z, \\ \dfrac{dz}{dt} = -a\,x - y - 1.1\,z - 2.7\,z^2 + x(y + 0.25\,z), \end{cases} \tag{26}$$

and

$$\begin{cases} \dfrac{dx}{dt} = y, \\ \dfrac{dy}{dt} = z, \\ \dfrac{dz}{dt} = -a\,x - y - 1.1\,z - 2.59\,z^2 + xy, \end{cases} \tag{27}$$

respectively. For these three systems, according to the signs of W_1, the Hopf bifurcations occur at $a = 1.1$ are all subcritical.

Taking a as the parameter, the bifurcation diagrams and Lyapunov exponents are plotted for the above three systems, see Figures 5–7, respectively. The selected initial conditions are the same: $x(0) = z(0) = 0, y(0) = -1.5$.

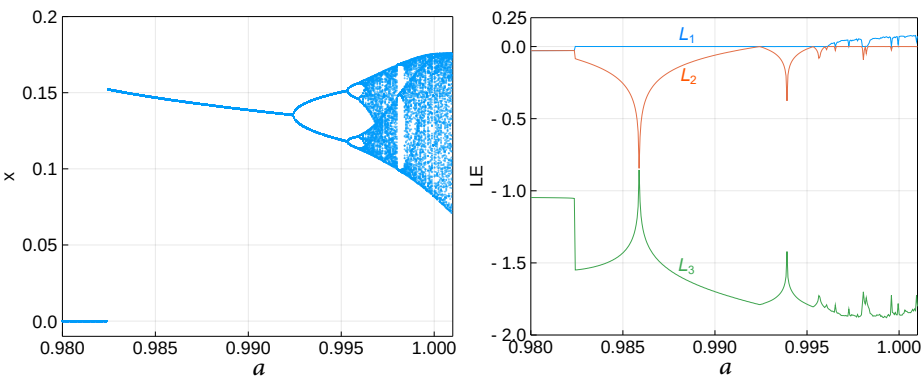

(**a**) (**b**)

Figure 5. (**a**) Bifurcation diagram, and (**b**) Lyapunov exponents spectrum versus a of system (25).

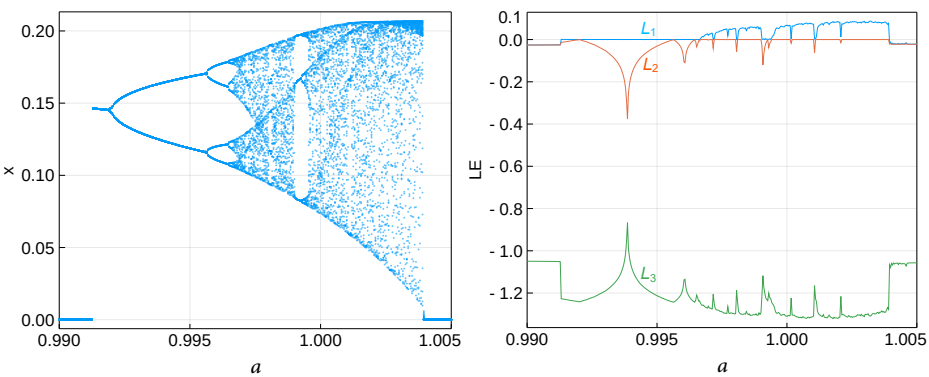

(**a**) (**b**)

Figure 6. (**a**) Bifurcation diagram, and (**b**) Lyapunov exponents spectrum versus a of system (26).

Based on Figures 5–7, the following observations can be made:

1. With the increase in parameter a, these systems share the same hidden mechanism: stable equilibrium $\rightarrow$ hidden period-1 limit cycles $\rightarrow$ period doubling cascades $\rightarrow$ hidden chaos.

2. There are several jump discontinuities for some curves in the bifurcation diagrams.

3. For $a = 1$, these systems exhibit hidden chaotic attractors as the unique equilibrium is stable.

4. By selecting $a = 1$ in systems (25)–(27), system (27) is the most elegant in the sense that: it has three coefficients in the form of ± 1 and only two nonlinearities; it is not on the list of [42].

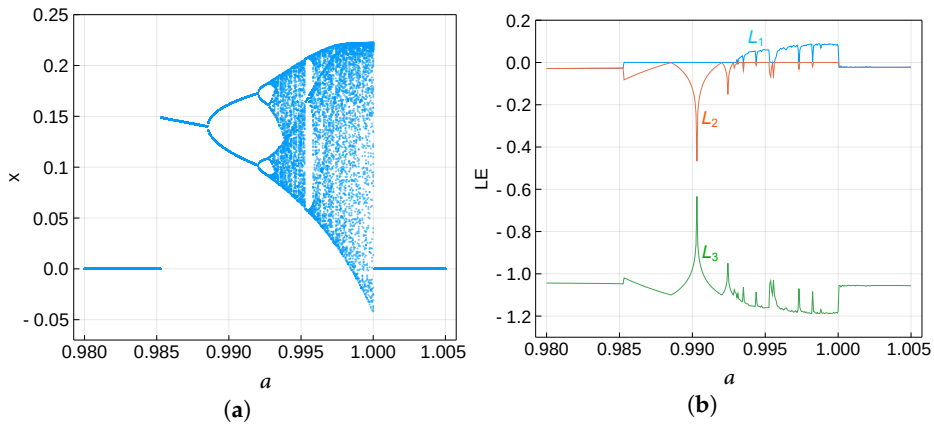

Figure 7. (**a**) Bifurcation diagram, and (**b**) Lyapunov exponents spectrum versus a of system (27).

8. Hidden Chaotic Attractor

Based on the bifurcation analysis, it is of interest to study the following system

$$\begin{cases} \dfrac{dx}{dt} = y, \\ \dfrac{dy}{dt} = z, \\ \dfrac{dz}{dt} = -x - y - 1.1\,z - 2.59\,z^2 + xy. \end{cases} \tag{28}$$

As shown in the Figure 8, the system generates a hidden chaotic attractor and a point attractor (located at the origin). The cross sections of the basins of attraction of the attractors in the three coordinate planes are shown in Figure 9. The initial condition for these figures is $(x(0), y(0), z(0)) = (0, -1.5, 0)$.

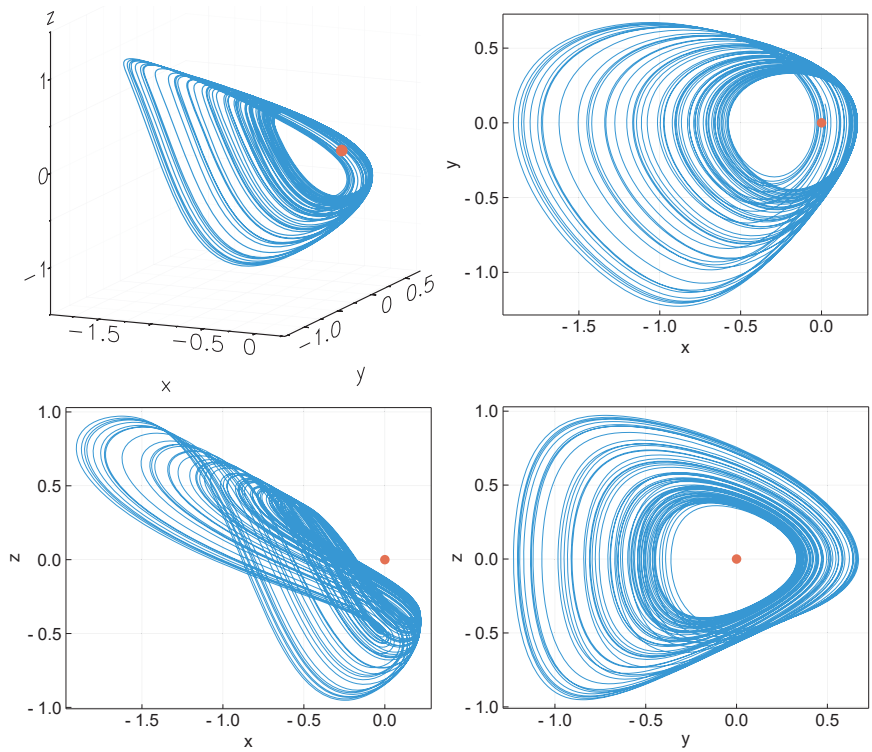

Figure 8. A 3D view of the hidden chaotic attractor (in blue) and point attractor (in red) of system (28) and its various projections. Initial condition that realizes the hidden hidden chaotic attractor: $(x(0), y(0), z(0)) = (0, -1.5, 0)$.

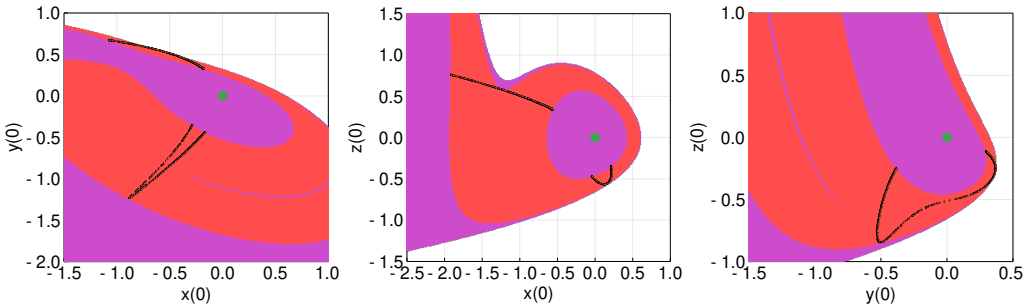

Figure 9. Cross sections of the basins of attraction of the two coexisting attractors in the coordinate planes: $z(0) = 0$ (**left**); $y(0) = 0$ (**center**); $x(0) = 0$ (**right**). Initial conditions in the white regions lead to unbounded orbits, those in the red regions lead to the hidden chaotic attractor, and those in the purple regions lead to the stable equilibrium located at the origin.

The Lyapunov exponents of the attractor are $(L_1, L_2, L_3) = (0.07977, 0, -1.1795)$, thus the Kaplan–Yorke dimension is $D_{KY} = 2.0677$. This confirms that system (28) is dissipative with a hidden chaotic attractor.

9. Circuit Realization

Using electronic circuits to simulate chaotic systems is an effective way to investigate their dynamics. The realization of chaotic electronic circuits based on theoretical models is an important topic relating to practical applications. Such circuits are a crucial part of various chaos-based applications, including image encryption schemes and path-planning generators for autonomous mobile robots [80–82].

An electronic circuit for system (28) is shown in Figure 10. It consists of three operational amplifiers (op-amps) U_1 to U_3 for three integration channels, two op-amps U_4 and U_5 for the inverting amplifiers, and two analog multipliers U_6 and U_7 (using AD633 with an implied voltage factor of 1) for the two quadratic nonlinearities. All the op-amps are TL082 ICs powered at ± 15 V.

By applying Kirchhoff's circuit laws, the corresponding circuital equations of the circuit can be written as follows:

$$\begin{cases} \dfrac{dX}{dt} = \dfrac{1}{RC_1}\left(\dfrac{R}{R_1}Y\right) \\ \dfrac{dY}{dt} = \dfrac{1}{RC_2}\left(\dfrac{R}{R_2}Z\right) \\ \dfrac{dZ}{dt} = \dfrac{1}{RC_3}\left(-\dfrac{R}{R_3}X - \dfrac{R}{R_4}Y - \dfrac{R}{R_5}Z - \dfrac{R}{R_6}Z^2 + \dfrac{R}{R_7}XY\right), \end{cases} \tag{29}$$

where the phase space variables X, Y, and Z represent the output voltages of U_4, U_5 and U_3. Setting $R/R_1 = R/R_2 = R/R_4 = R/R_7 = 1$, $R/R_3 = 1$, $R/R_5 = 1.1$, $R/R_6 = 2.59$ and $C_1 = C_2 = C_3$, it is easy to see that system (29) is orbitally equivalent to system (28)

Let $C_1 = C_2 = C_3 = 100$nF, $R = R_1 = R_2 = R_3 = R_4 = R_7 = 100\,\text{k}\Omega$, $R_5 = 90.91\,\text{k}\Omega$, $R_6 = 38.61\,\text{k}\Omega$ and $R_8 = R_9 = R_{10} = R_{11} = 10\,\text{k}\Omega$. By using OrCAD-PSpice, the various 2D projections of the hidden chaotic attractor of system (29) are shown in Figure 11. The obtained results are consistent with the numerical results in Figure 8.

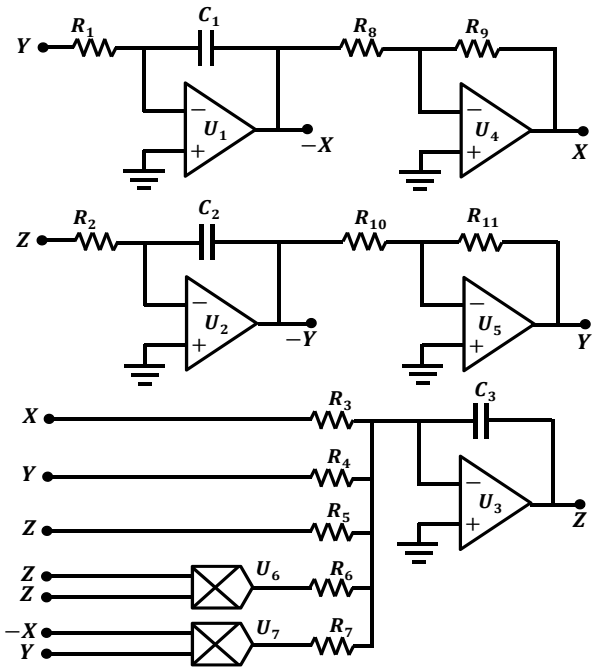

Figure 10. Circuital implementation of the hidden chaotic system (28) with a stable equilibrium at the origin.

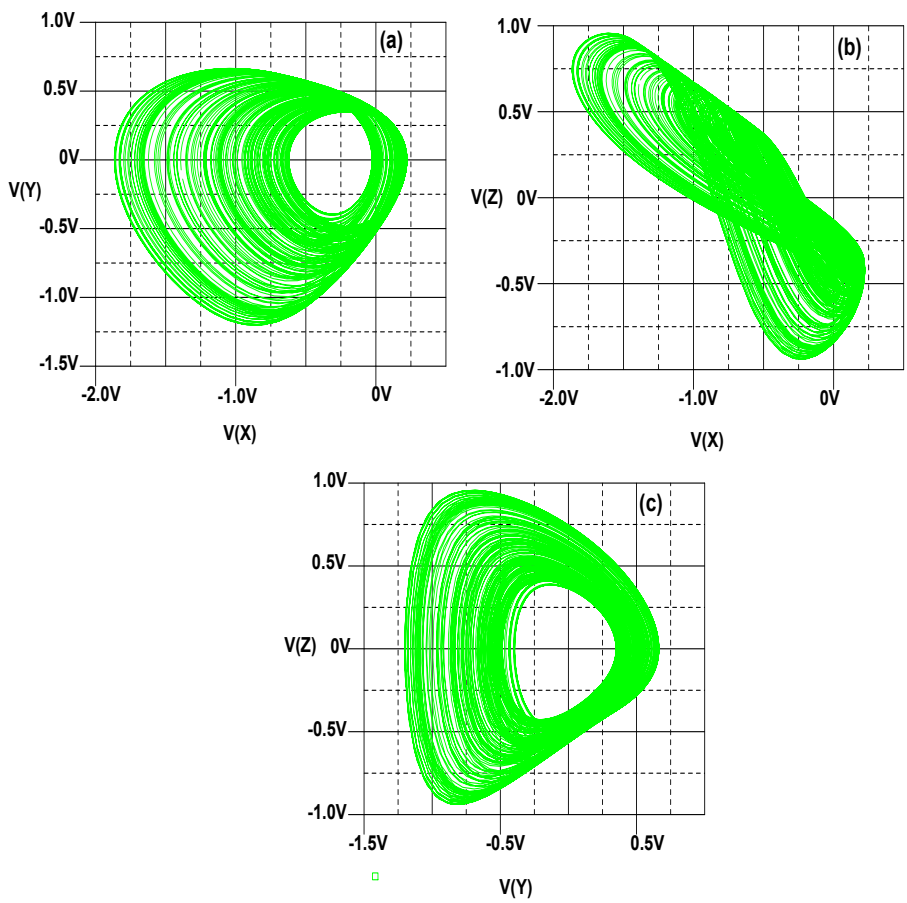

Figure 11. Hidden chaotic attractor of system (29): (**a**) X-Y projection of the attractor, (**b**) X-Z projection of the attractor, and (**c**) Y-Z projection.

10. Conclusions

This work is mainly about a two-parameter family of 3D quadratic jerk systems with complex dynamics. In Section 2, the analysis of a Hopf bifurcation is carried out for a general five-parameter family of 3D quadratic jerk systems, which includes the two-parameter family and the hidden chaotic system SE_1 of [42]. The remaining sections are devoted to the two-parameter family. The nonchaotic parameter region is found to reduce the complexity of finding chaotic attractors. Depending on the combination of the two parameters, the jerk system can exhibit self-excited chaotic attractors with an unstable equilibrium, or hidden chaotic attractors with a stable equilibrium. Some numerical methods are used for finding these attractors, such as phase portraits, Lyapunov exponents, bifurcation diagrams, and cross sections. The transition from regular attractors to chaotic attractors is via period-doubling cascades of limit cycles. For the self-excited case, the initial limit cycles are generated by the supercritical Hopf bifurcation. For the hidden case (associated with the subcritical Hopf bifurcation), the initial limit cycles are hidden and are not generated by the subcritical Hopf bifurcation. Finally, an electric circuit is designed to validate the existence of a hidden chaotic attractor. The hidden chaotic system (28) is algebraically elegant, which expands the list of hidden chaotic jerk systems.

Author Contributions: Conceptualization, M.L.; methodology, B.S.; software, N.W. and I.A.; writing—original draft preparation, M.L.; writing—review and editing, B.S.; supervision, B.S.; project administration, B.S.; funding acquisition, B.S. All authors have read and agreed to submit the manuscript.

Funding: This research was funded by Shandong Provincial Natural Science Foundation, China (ZR2018MA025).

Institutional Review Board Statement: Not applicable.

Informed Consent Statement: Not applicable.

Data Availability Statement: The data presented in this study are available on request from authors.

Conflicts of Interest: The authors declare no conflict of interest.

References

1. Thompson, J.M.T.; Stewart, H.B. *Nonlinear Dynamics and Chaos*; Wiley: Chichester, UK, 2002.
2. Wiggins, S. *Introduction to Applied Nonlinear Dynamical Systems and Chaos*; Springer: New York, NY, USA, 1990.
3. Mangiarotti, S.; Peyre, M.; Zhang, Y.; Huc, M.; Roger, F.; Kerr, Y. Chaos theory applied to the outbreak of COVID-19: An ancillary approach to decision making in pandemic context. *Epidemiol Infect.* **2020**, *148*, 95. [CrossRef] [PubMed]
4. Scheck, F. *Mechanics: From Newton's Laws to Deterministic Chaos*; Springer: Berlin, Germany, 2012.
5. Toker, D.; Sommer, F.T.; D'Esposito, M. A simple method for detecting chaos in nature. *Commun. Biol.* **2020**, *3*, 11. [CrossRef]
6. Volos, C.K.; Kyprianidis, I.M.; Stouboulos I.N. Experimental demonstration of a chaotic cryptographic scheme. *WSEAS Trans. Circ. Syst.* **2006**, *5*, 1654–1661.
7. Zaher, A.A.; Abu-Rezq, A. On the design of chaos-based secure communication systems. *Commun. Nonlinear Sci. Numer. Simulat.* **2011**, *16*, 3721–3737. [CrossRef]
8. Wei, Z.C.; Sprott, J.C.; Chen, H. Elementary quadratic chaotic flows with a single non-hyperbolic equilibrium. *Phys. Lett. A* **2015**, *379*, 2184–2187. [CrossRef]
9. Leonov, G.A.; Kuznetsov, N.V. Hidden attractors in dynamical systems. From hidden oscillations in Hilbert-Kolmogorov, Aizerman, and Kalman problems to hidden chaotic attractor in Chua circuits. *Int. J. Bifurc. Chaos* **2013**, *23*, 1330002. [CrossRef]
10. Lorenz, E.N. Deterministic nonperiodic flow. *J. Atmos. Sci.* **1963**, *20*, 130–141. [CrossRef]
11. Rössler, O.E. An equation for continuous chaos. *Phys. Lett. A* **1976**, *57*, 397–398. [CrossRef]
12. Chua, L.O. The genesis of Chua's circuit. *AEÜ* **1992**, *46*, 250–257.
13. Silva, C.P. Shil'nikov's theorem-a tutorial. *IEEE Trans. Circuits Syst. I Reg. Pap.* **1993**, *40*, 675–682. [CrossRef]
14. Tchitnga, R.; Nguazon, T.; Fotso, P.H.L.; Gallas, J.A.C. Chaos in a single Op-Amp based jerk circuit. *IEEE Trans. Circuits Syst. II Express Briefs* **2016**, *63*, 239–243. [CrossRef]
15. Chen, G.R.; Ueda, T. Yet another chaotic attractor. *Int. J. Bifurc. Chaos* **1999**, *9*, 1465–1466. [CrossRef]
16. Lü, J.H.; Chen, G.R. A new chaotic attractor coined. *Int. J. Bifurc. Chaos* **2002**, *12*, 659–661. [CrossRef]
17. Sprott, J.C. *Elegant Chaos: Algebraically Simple Chaotic Flows*; World Scientific: Singapore, 2010.
18. Kuznetsov, N.V.; Leonov, G.A.; Vagaitsev, V.I. Analytical-numerical method for attractor localization of generalized Chua's system. *IFAC Proc.* **2010**, *43*, 29–33. [CrossRef]

19. Leonov, G.A.; Kuznetsov, N.V.; Vagaitsev, V.I. Localization of hidden Chua's attractors. *Phys. Lett. A* **2011**, *375*, 2230–2233. [CrossRef]
20. Kuznetsov, N.V. Hidden attractors in fundamental problems and engineering models. A short survey. *Lect. Notes Electr. Eng.* **2016**, *371*, 13–25.
21. Stankevich, N.V.; Kuznetsov, N.V.; Leonov, G.A.; Chua, L.O. Scenario of the birth of hidden attractors in the Chua circuit. *Int. J. Bifurc. Chaos* **2017**, *27*, 1730038. [CrossRef]
22. Zhao, H.T.; Lin, Y.P.; Dai, Y.X. Hidden attractors and dynamics of a general autonomous van der Pol–Duffing oscillator. *Int. J. Bifurc. Chaos* **2014**, *24*, 1450080. [CrossRef]
23. Jafari, S.; Sprott, J.C.; Golpayegani, S.M.R.H. Elementary quadratic chaotic flows with no equilibria. *Phys. Lett. A* **2013**, *377*, 699–702. [CrossRef]
24. Jafari, S.; Sprott, J.C. Simple chaotic flows with a line equilibrium. *Chaos Solitons Fractals* **2013**, *57*, 79–84. [CrossRef]
25. Jafari, S.; Sprott, J.C.; Nazarimehr, F. Recent new examples of hidden attractors. *Eur. Phys. J. Spec. Top.* **2015**, *224*, 1469–1476. [CrossRef]
26. Jafari, S.; Sprott, J.C.; Molaie, M. A simple chaotic flow with a plane of equilibria. *Int. J. Bifurcat. Chaos* **2016**, *26*, 1650098. [CrossRef]
27. Jafari, S.; Sprott, J.C.; Pham, V.T.; Volos, C.; Li, C.B. Simple chaotic 3D flows with surfaces of equilibria. *Nonlinear Dyn.* **2016**, *86*, 1349–1358. [CrossRef]
28. Sprott, J.C. Strange attractors with various equilibrium types. *Eur. Phys. J. Spec. Top.* **2015**, *224*, 1409–1419. [CrossRef]
29. Bao, B.C.; Xu, L.; Wang, N.; Bao, H.; Xu, Q.; Chen, M. Third-order RLCM-four-elements-based chaotic circuit and its coexisting bubbles. *AEÜ-Int. J. Electron. Commun.* **2018**, *94*, 26–35. [CrossRef]
30. Danca, M.F.; Kuznetsov, N. Hidden strange nonchaotic attractors. *Mathematics* **2021**, *9*, 652. [CrossRef]
31. Jafari, M.A.; Mliki, E.; Akgul, A.; Pham, V.T.; Kingni, S.T.; Wang, X.; Jafari, S. Chameleon: The most hidden chaotic flow. *Nonlinear Dyn.* **2017**, *88*, 2303–2317. [CrossRef]
32. Pham, V.T.; Vaidyanathan, S.; Volos, C.; Kapitaniak, T. (Eds.) *Nonlinear Dynamical Systems with Self-Excited and Hidden Attractors*; Springer: Cham, Switzerland, 2018.
33. Wang, N.; Zhang, G.S.; Kuznetsov, N.V.; Bao, H. Hidden attractors and multistability in a modified Chua's circuit. *Commun. Nonlinear Sci. Numer. Simul.* **2021**, *92*, 105494. [CrossRef]
34. Pham, V.T.; Volos, C.; Jafari, S.; Kapitaniak, T. Coexistence of hidden chaotic attractors in a novel no-equilibrium system. *Nonlinear Dyn.* **2017**, *87*, 2001–2010. [CrossRef]
35. Shahzad, M.; Pham, V.T.; Ahmad, M.A.; Jafari, S.; Hadaeghi, F. Synchronization and circuit design of a chaotic system with coexisting hidden attractors. *Eur. Phys. J. Spec. Top.* **2015**, *224*, 1637–1652. [CrossRef]
36. Tamba, V.K.; Pham, V.T.; Duy V.H.; Jafari, S.; Alsaadi, F.E.; Alsaadi, F.E. Dynamic system with no equilibrium and its chaos anti-synchronization. *Automatika* **2018**, *59*, 35–42. [CrossRef]
37. Tutueva, A.V.; Karimov, T.I.; Nepomuceno, E.G.; Butusov, D.N. Detection of hidden oscillations in systems without equilibrium. *Int. J. Bifurc. Chaos* **2021**, *31*, 2150043. [CrossRef]
38. Zhang, S.; Wang, X.P.; Zeng, Z.G. A simple no-equilibrium chaotic system with only one signum function for generating multidirectional variable hidden attractors and its hardware implementation. *Chaos* **2020**, *30*, 053129. [CrossRef] [PubMed]
39. Zhou, W.; Wang, G.Y.; Shen, Y.R.; Yuan, F.; Yu, S.M. Hidden coexisting attractors in a chaotic system without equilibrium point. *Int. J. Bifurc. Chaos* **2018**, *28*, 1830033. [CrossRef]
40. Bao, B.C.; Hu, F.W.; Chen, M.; Xu, Q.; Yu, Y.J. Self-excited and hidden attractors found simultaneously in a modified Chua's circuit. *Int. J. Bifurc. Chaos* **2015**, *25*, 1550075. [CrossRef]
41. Deng, Q.L.; Wang, C.H. Multi-scroll hidden attractors with two stable equilibrium points. *Chaos* **2019**, *29*, 093112. [CrossRef]
42. Molaie, M.; Jafari, S.; Sprott, J.C.; Golpayegani, S.M.R.H. Simple chaotic flows with one stable equilibrium. *Int. J. Bifurc. Chaos* **2013**, *23*, 1350188. [CrossRef]
43. Munmuangsaen, B.; Srisuchinwong, B. A hidden chaotic attractor in the classical Lorenz system. *Chaos Solitons Fractals* **2018**, *107*, 61–66. [CrossRef]
44. Wang, X.; Pham, V.T.; Jafari, S.; Volos, C.; Munoz-Pacheco, J.M.; Tlelo-Cuautle, E. A new chaotic system with stable equilibrium: From theoretical model to circuit implementation. *IEEE Access* **2017**, *5*, 8851–8858. [CrossRef]
45. Wei, Z.C.; Yang, Q.G. Dynamical analysis of a new autonomous 3-D chaotic system only with stable equilibria. *Nonlin Anal. Real World Appl.* **2011**, *12*, 106–118. [CrossRef]
46. Wei, Z.C.; Wang, Z. Chaotic behavior and modified function projective synchronization of a simple system with one stable equilibrium. *Kybernetika* **2013**, *49*, 359–374.
47. Barati, K.; Jafari, S.; Sprott, J.C.; Pham, V.T. Simple chaotic flows with a curve of equilibria. *Int. J. Bifurc. Chaos* **2016**, *26*, 1630034. [CrossRef]
48. Gotthans, T.; Sprott, J.C.; Petrzela, J. Simple chaotic flow with circle and square equilibrium. *Int. J. Bifurc. Chaos* **2016**, *26*, 1650137. [CrossRef]
49. Pham, V.T.; Volos, C.; Kapitaniak, T.; Jafari, S.; Wang, X. Dynamics and circuit of a chaotic system with a curve of equilibrium points. *Int. J. Electron.* **2018**, *105*, 385–397. [CrossRef]

50. Pham, V.T.; Volos, C.; Jafari, S.; Wei, Z.C.; Wang, X. Constructing a novel no-equilibrium chaotic system. *Int. J. Bifurc. Chaos* **2014**, *24*, 1450073. [CrossRef]
51. Pham, V.T.; Jafari, S.; Kapitaniak, T. Constructing a chaotic system with an infinite number of equilibrium points. *Int. J. Bifurc. Chaos* **2016**, *26*, 1650225. [CrossRef]
52. Pham, V.T.; Jafari, S.; Kapitaniak, T.; Volos, C.; Kingni, S.T. Generating a chaotic system with one stable equilibrium. *Int. J. Bifurc. Chaos* **2017**, *27*, 1750053. [CrossRef]
53. Joshi, M.; Ranjan, A. An autonomous simple chaotic jerk system with stable and unstable equilibria using reverse sine hyperbolic functions. *Int. J. Bifurc. Chaos* **2020**, *30*, 2050070. [CrossRef]
54. Kingni, S.T.; Kuiate, G.F.; Tamba, V.K.; Pham, V.T.; Hoang, D.V. Self-excited and hidden attractors in an autonomous Josephson jerk oscillator: Analysis and its application to text encryption. *J. Comput. Nonlinear Dynam.* **2019**, *14*, 071004. [CrossRef]
55. Li, C.B.; Sprott, J.C.; Joo-Chen Thio, W.; Gu, Z.Y. A simple memristive jerk system. *IET Circuits Devices Syst.* **2021**, *15*, 388–392. [CrossRef]
56. Zhang, S.; Zeng, Y.C. A simple Jerk-like system without equilibrium: Asymmetric coexisting hidden attractors, bursting oscillation and double full Feigenbaum remerging trees. *Chaos Solitons Fractals* **2019**, *120*, 25–40. [CrossRef]
57. Danca, M.F. Hidden chaotic attractors in fractional-order systems. *Nonlinear Dyn.* **2017**, *89*, 577–586. [CrossRef]
58. Liu, T.M.; Ya, H.Z.; Banerjee, S.; Mou, J. A fractional-order chaotic system with hidden attractor and self-excited attractor and its DSP implementation. *Chaos Solitons Fractals* **2021**, *145*, 110791. [CrossRef]
59. Li, C.B.; Sprott, J.C. Multistability in the Lorenz system: A broken butterfly. *Int. J. Bifurcat. Chaos* **2014**, *24*, 1450131. [CrossRef]
60. Chudzik, A.; Perlikowski, P.; Stefanski, A.; Kapitaniak, T. Multistability and rare attractors in van der Pol-Duffing oscillator. *Int. J. Bifurc. Chaos* **2011**, *21*, 1907–1912. [CrossRef]
61. He, S.B.; Natiq, H.; Mukherjee, S. Multistability and chaos in a noise-induced blood flow. *Eur. Phys. J. Spec. Top.* **2021**, *230*, 1525–1533. [CrossRef]
62. Kapitaniak, T.; Leonov, G.A. Multistability: Uncovering hidden attractors. *Eur. Phys. J. Spec. Top.* **2015**, *224*, 1405–1408. [CrossRef]
63. Tagne, R.L.M.; Kengne, J.; Nguomkam Negou, A. Multistability and chaotic dynamics of a simple Jerk system with a smoothly tuneable symmetry and nonlinearity. *Int. J. Dyn. Control* **2019**, *7*, 476–495. [CrossRef]
64. Natiq, H.; Kamel Ariffin, M.R.; Asbullah, M.A.; Mahad, Z.; Najah, M. Enhancing chaos complexity of a plasma model through power input with desirable random features. *Entropy* **2021**, *23*, 48. [CrossRef] [PubMed]
65. Lai, Q.; Norouzi B.; Liu, F. Dynamic analysis, circuit realization, control design and image encryption application of an extended Lü system with coexisting attractors. *Chaos Solitons Fractals* **2018**, *114*, 230–245. [CrossRef]
66. Peng, G.Y.; Min, F.H. Multistability analysis, circuit implementations and application in image encryption of a novel memristive chaotic circuit. *Nonlinear Dyn.* **2017**, *90*, 1607–1625. [CrossRef]
67. Bao, J.H.; Liu, Y.J. Multistability and bifurcations in a 5D segmented disc dynamo with a curve of equilibria. *Adv. Differ. Equ.* **2019**, *2019*, 345. [CrossRef]
68. Rajagopal, K.; Akgul, A.; Moroz, I.M.; Wei, Z.C.; Jafari, S.; Hussain, I. A simple chaotic system with topologically different attractors. *IEEE Access* **2019**, *7*, 89936–89947. [CrossRef]
69. Singh, J.P.; Roy, B.K.; Kuznetsov, N.V. Multistability and hidden attractors in the dynamics of permanent magnet synchronous motor. *Int. J. Bifurc. Chaos* **2019**, *29*, 1950056. [CrossRef]
70. Njitacke, Z.T.; Kengne, J.; Kamdjeu Kengne, L. Antimonotonicity, chaos and multiple coexisting attractors in a simple hybrid diode-based jerk circuit. *Chaos Solitons Fractals* **2017**, *105*, 77–91. [CrossRef]
71. Zhang, Y.Z.; Liu, Z.; Wu, H.G.; Chen, S.Y.; Bao, B.C. Extreme multistability in memristive hyper-jerk system and stability mechanism analysis using dimensionality reduction model. *Eur. Phys. J. Spec. Top.* **2019**, *228*, 1995–2009. [CrossRef]
72. Chen, H.; He, S.B.; Pano Azucena, A.D.; Yousefpour, A.; Jahanshahi, H.; López, M.A.; Alcaraz, R. A multistable chaotic jerk system with coexisting and hidden attractors: Dynamical and complexity analysis, FPGA-based realization, and chaos stabilization using a robust controller. *Symmetry* **2020**, *12*, 569. [CrossRef]
73. Faghani, Z.; Nazarimehr, F.; Jafari, S.; Sprott J.C. A new category of three-dimensional chaotic flows with identical eigenvalues. *Int. J. Bifurc. Chaos* **2020**, *30*, 2050026. [CrossRef]
74. Rajagopal, K.; Kingni, S.T.; Kom, G.H.; Pham, V.T.; Karthikeyan, A.; Jafari, S. Self-excited and hidden attractors in a simple chaotic jerk system and in its time-delayed form: Analysis, electronic implementation, and synchronization. *J. Korean Phys. Soc.* **2020**, *77*, 145–152. [CrossRef]
75. Sprott, J.C. A proposed standard for the publication of new chaotic systems. *Int. J. Bifurc. Chaos* **2011**, *21*, 2391–2394. [CrossRef]
76. Sang, B. Hopf bifurcation formulae and applications to the Genesio-Tesi system. *J. Nonlinear Funct. Anal.* **2019**, *2019*, 34.
77. Liu, W.M. Criterion of Hopf bifurcation without using eigenvalues. *J. Math. Anal. Appl.* **1994**, *182*, 250–256. [CrossRef]
78. Wang, Q.L.; Liu, Y.R.; Chen, H.B. Hopf bifurcation for a class of three-dimensional nonlinear dynamic systems. *Bull. Sci. Math.* **2010**, *134*, 786–798. [CrossRef]
79. Sang, B. The Hopf bifurcations in the permanent magnet synchronous motors. *J. Nonlinear Model. Anal.* **2021**, *3*, 179–191.
80. Volos, C.K.; Kyprianidis, I.M.; Stouboulos, I.N. A chaotic path planning generator for autonomous mobile robots. *Robot. Auton. Syst.* **2012**, *60*, 651–656. [CrossRef]

81. Chen, G.R.; Ueda, T. *Chaos in Circuits and Systems*; World Scientific: Singapore, 2002.
82. Wang, N.; Zhang, G.S.; Bao, H. Bursting oscillations and coexisting attractors in a simple memristor-capacitor-based chaotic circuit. *Nonlinear Dyn.* **2019**, *97*, 1477–1494. [CrossRef]